LA-UR-93-0045

LA-UR--93-0045

DE93 007354

Los Alamos National Laboratory is operated by the University of California for the United States Department of Energy under contract W-7405-ENG-36

TITLE: *COMPUTATIONAL MODELING OF "MAGO" AND OTHER MAGNETIZED TARGET FUSION CONCEPTS*

AUTHOR(S): *I. R. LINDEMUTH, R. C. KIRKPATRICK, R. E. REINOVSKY, P. T. SHEEHEY, R. S. THURSTON, F. J. WYSOCKI*

SUBMITTED TO: *SIXTH INTERNATIONAL CONFERENCE ON MEGAGAUSS MAGNETIC FIELD GENERATION AND RELATED TOPICS NOV. 9-11, 1992, ALBUQUERQUE, NM*

MASTER

Los Alamos

Los Alamos National Laboratory
Los Alamos, New Mexico 87545

FORM NO 836 R4
ST NO 2629 5/81

COMPUTATIONAL MODELING OF "MAGO" AND OTHER MAGNETIZED TARGET FUSION CONCEPTS

I. R. Lindemuth, R. C. Kirkpatrick, R. E. Reinovsky,
P. T. Sheehey, R. S. Thurston, F. J. Wysocki
Los Alamos National Laboratory
Los Alamos, New Mexico 87545, USA

1. INTRODUCTION

One of the most appropriate applications of high current, high energy pulsed power is as a driver for a thermonuclear fusion target [1,2]. We are considering the applications of pulsed power technology to an area of fusion research we have named magnetized target fusion (MTF), to distinguish it from the more conventional magnetic fusion energy (MFE) research and inertial confinement fusion (ICF). MTF is a relatively untried approach to fusion ignition which uses a magnetic field within a fusion target to suppress thermal conduction losses while retaining the implosion heating and inertial confinement advantages of conventional ICF. MTF includes, but is not limited to, such previous endeavors as the Sandia Φ target, imploding liner fusion, and impact fusion.

The basic principles of MTF have previously been reported. Using a simple target model [3] which included such phenomena as magnetic back-pressure on an imploding pusher, magnetic reduction of thermal conductivity, magnetic diffusion, and Ohmic heating as well as the usual hydrodynamic and radiation phenomena, new regions in parameter space where significant thermonuclear fuel burn-up can occur were identified. When compared with ICF, the new regions are characterized by very low fuel densities, very low implosion velocities, and, most importantly, driver requirements reduced by several orders of magnitude. The simple model was extended to include a cold fuel layer [4], and it was found that high gain was possible in a new parameter space. Although we have used simple models to explore the parameter space appropriate for MTF, we have confirmed the basic results of our simple models using more sophisticated computational tools [3,5]

Operating in a density and time parameter range intermediate to ICF and MFE, MTF appears to have distinct advantages over both of the more conventional approaches. MTF is not merely the addition of a magnetic field to an ICF target. The lower densities of MTF imply a larger target for the same fuel mass. The larger targets and lower implosion velocities imply more massive pushers, which in turn lead to longer dwell and burn times. Because MTF represents an approach to an adiabatic compression, driver pulse shaping is not required. The magnetic field which is compressed along with the fuel may reach a value whereby charged particle energy deposition is enhanced.

MTF does not require magnetic confinement such as required in MFE. In general, the plasma β (β=plasma pressure/magnetic pressure) is much greater than unity and most of the plasma pressure is supported by the confining pusher. Because the fuel is wall-confined, many of the instabilities which are deleterious to MFE are not be expected to be as severe.

Because wall confinement is adequate, simple magnetic field topologies can be considered, leading to easier plasma formation techniques.

An MTF system requires two elements: (a) a target implosion driver; (b) a means of preheating and magnetizing the thermonuclear fuel prior to implosion. Although lasers and particle beam drivers optimized for unpreheated, unmagnetized targets are probably not appropriate for MTF at its extremes, there is a continuum betwen conventional target space and MTF space, suggesting a possible role for existing target drivers. However, because of the reduced driver power and intensity requirements, MTF permits a complete rethinking of the entire driver/target configuration. Novel 100-MJ-class disk flux compression generators [6,7] make it possible to consider direct magnetic implosion [1] of fusion targets in a energy-velocity space simply inaccessible by any other laboratory means [8]; such energy sources appear ideal for MTF [2].

One possible way to obtain a preheated and magnetized plasma suitable for subsequent implosion is the "MAGO" concept [9]. The unique MAGO discharge consists of a two chambers, with electrical current flowing in one chamber accelerating plasma flow into an implosion chamber. Up to 4 x 10^{13} D-T neutrons have been produced in the MAGO discharge.

In this paper, we discuss our computational modeling of MAGO. Our objectives are to characterize the plasma, compare with the limited diagnostics available, and to understand the neutron production. We also discuss, briefly, some other possible means for creating a magnetized plasma.

2. COMPUTATIONAL CONSIDERATIONS

Most of our computational modeling has been performed with the two-dimensional computer code MHRDR (Magneto-, Hydro-, Radiative Dynamics Research). MHRDR has been used most extensively to model the behavior of cryogenic deuterium fiber z-pinches [10,11].

Although MHRDR has an extensive diagnostic capability, it has limited geometric capability. Therefore, the MAGO geometry can be represented only approximately. Shown in Fig. 1 are the two MAGO geometries and the MHRDR approximation.

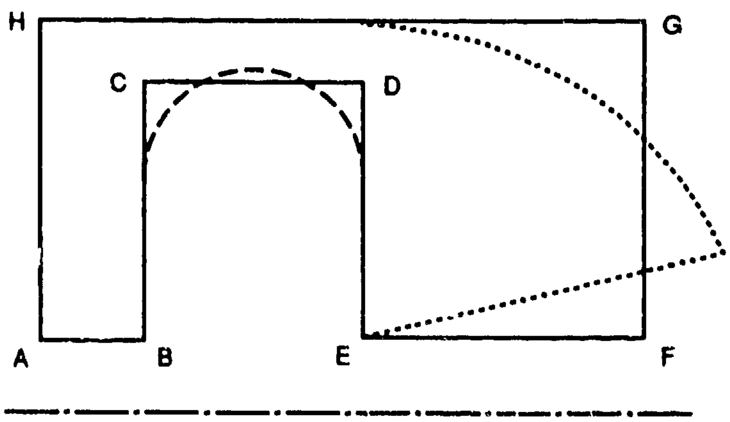

Fig. 1. The geometry used in the MHRDR computations (solid). Also shown are the two geomteries discussed in [9] (dashed, dashed + dotted). Boundary AB is an insulator, and all other boundaries are conductors. We have assumed that all data reported in [9] refers to the dashed geometry.

In principle, all gas within the discharge is initially at room temperature, although the presence of tritium may lead to a non-negligible initial ionization [12]. In MHRDR, if the gas is initially at room temperature, it will have a very high resistance through which no current will flow and the MAGO combined chamber will behave computationally like a fixed, large inductance. To establish conducting paths, we use an initial temperature of 2 eV for a small region adjacent to the insulator and for a small region at the center of the "nozzle" which connects the two chambers. The latter is used because the experimental results suggest that current initially flows in the nozzle as well as along the insulator. All other plasma is at room temperature, and all plasma has an initial deuterium density of 1.4 x 10^{-3} kg/m^3, corresponding to the D-T fill pressure of 5 torr. An initial, or bias, magnetic field is established by a 1.5 MA (1.7 MA in the experiment) current which surrounds the entire chamber.

The flux-compression generator system which provides the driving current for the experiment is represented computationally by a two loop fixed inductance electrical circuit with the loops separated by an opening switch. The inductance values and opening switch resistance are inferred from the paper [9].

The computations reported here use relatively coarse computational zones, with Δr=0.2 cm and Δz=0.25 cm.

3. COMPUTATIONAL RESULTS

The computations show a relatively weak inverse z-pinch forms at the insulator and moves radially outward. Concurrent with the inverse pinch, a dual current sheath drives gas in the nozzle towards the second chamber. Shown in Fig. 2 are density profiles in each region during the early phase of the discharge. In the inverse pinch (Fig. 2a), the shocked gas is heated to 1-2 eV. Very little current drives the inverse pinch. In the nozzle region (Fig. 2b), the low density plasma behind the weak axial shock is Ohmically heated to about 6 eV. Because of the relatively good electrical conductivity of the low density gas in the nozzle, approximately one-half of the current flows at the edge of the undisturbed gas at z=4 cm and one-half flows at the trailing edge of the axial shock at z=7 cm.

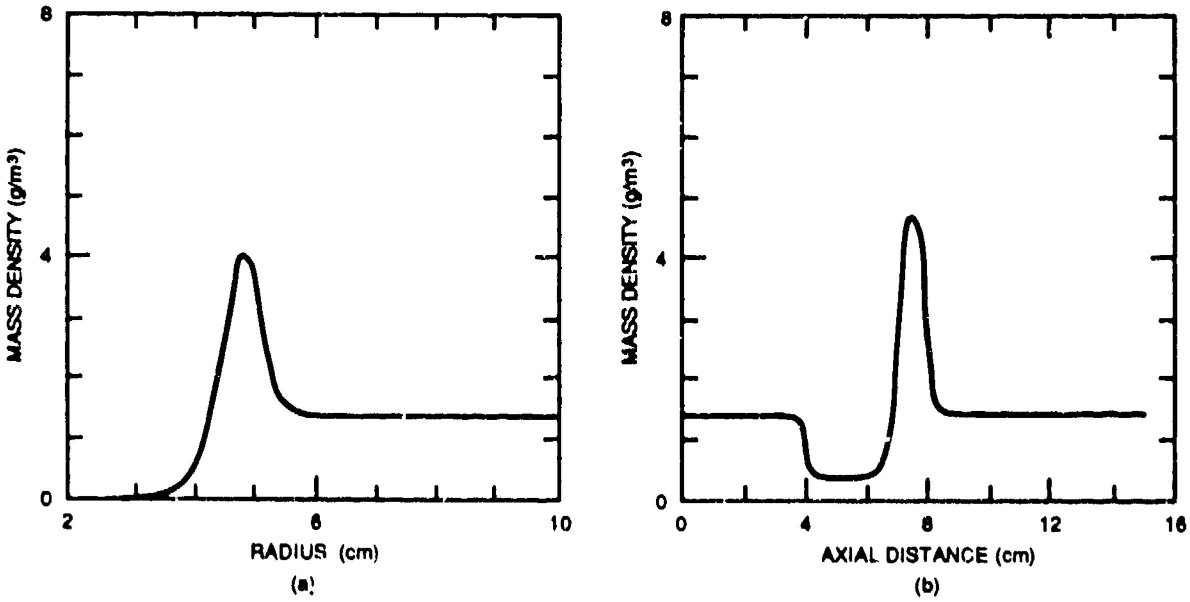

ig. 2. Mass density profiles at 1 μs. The radial profile (a) is taken in the middle of the acceleration chamber, half-way between boundaries AH and BC of Fig. 1. The axial profile (b) is taken in the middle of the nozzle, half-way between the boundaries CD and GH of Fig. 1.

The current which flows in the nozzle moves the gas ahead of it into the second chamber, compressing and heating it. Simultaneously, the inverse pinch moves radially outward until the nozzle region is encountered, at which time the flow becomes directed toward the nozzle. The mass which has accumulated in front of the inverse pinch is accelerated through the nozzle. Fig. 3 shows mass density contours which give the density distribution before (Fig. 3a) and after (Fig. 3b) the time of peak neutron production.

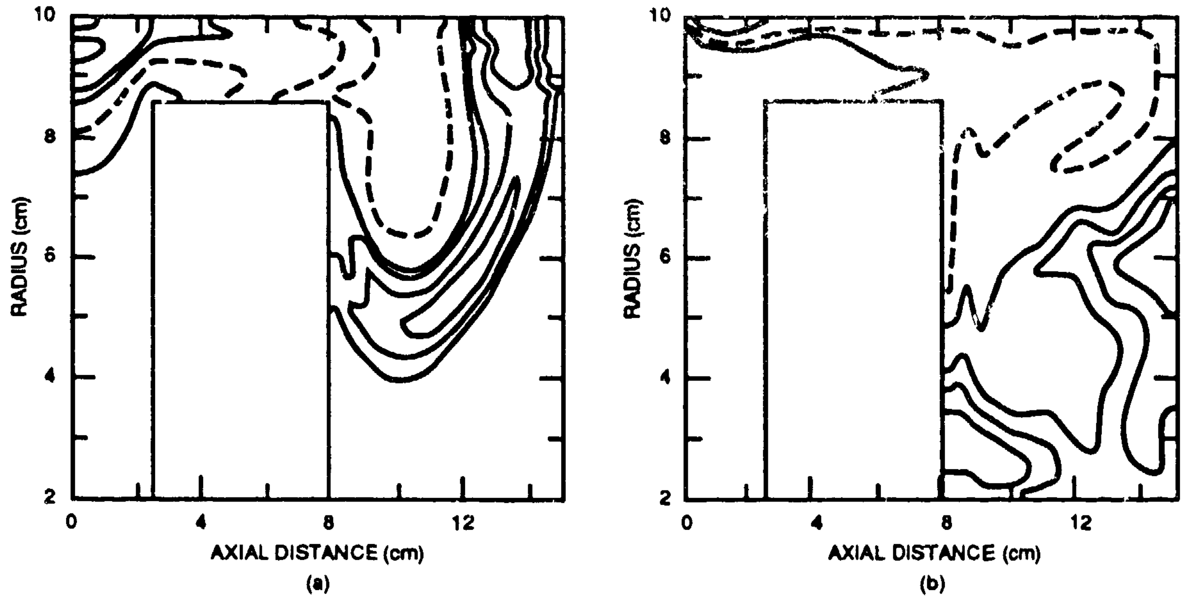

Fig. 3. Mass density contours in the r-z plane at 2 μs (a) and 3 μs (b). Contour values are chosen such that approximately 20% of the total mass is enclosed within each adjacent pair of solid contours. Also shown (dashed) is a low-density contour which encloses 95% of the total mass. Contour values (g/m^3) are: (a) 0.1, 0.44 (dotted), 1.8, 3.5, 5.2, 7.4; (b) 0.1, 0.51 (dotted), 1.3, 1.7, 3.2, 4.5.

In the experiment, plasma flow is diagnosed through the aid of dB/dt probes. Fig. 4 compares our computed integrated-dB/dt signals with the data and computations provided in the paper [9]. At the probe in the acceleration chamber (Fig. 4a), the integrated signal very closely follows the input current and indicates that less than 1 MA of the 4 MA applied by 1.5 μs is flowing in the inverse pinch. The relatively constant signal in the second chamber (Fig. 4b) until 2 μs indicates that most of the current is flowing in the nozzle region and that the plasma formed at the nozzle has sufficient electrical conductivity to prevent significant flux diffusion through the leading current sheath.

At 4 μs, the plasma, now located in the second chamber, has a thermal energy of 105 kJ and 617 kJ of magnetic energy is contained within the discharge chamber. The dominant heating mechanisms are compressional heating, with a total of 110 kJ of energy coupled to the plasma by reversible (pdV) and irreversible ("shock") heating. Ohmic heating is essentially negligible (5 kJ) The initial bias magnetic field sufficiently magnetizes the plasma so that very little energy (5 kJ) is lost to the surrounding walls by thermal conduction. Radiation losses for the plasma, assumed to be pure deuterium, are also negligible (3 kJ). A peak kinetic energy of 43 kJ occurs at 2.4 μs.

Peak neutron emission occurs in the computations at 2.5 μs. The neutrons are emitted by a toroidal volume surrounding the central conductor and also surrounding the bulk of the plasma, which has been compressed against the central conductor by essentially a z-pinch (Fig. 3a). The computed location of the neutron emitting region is consistent with the neutron "shadowgraph" obtained experimentally.

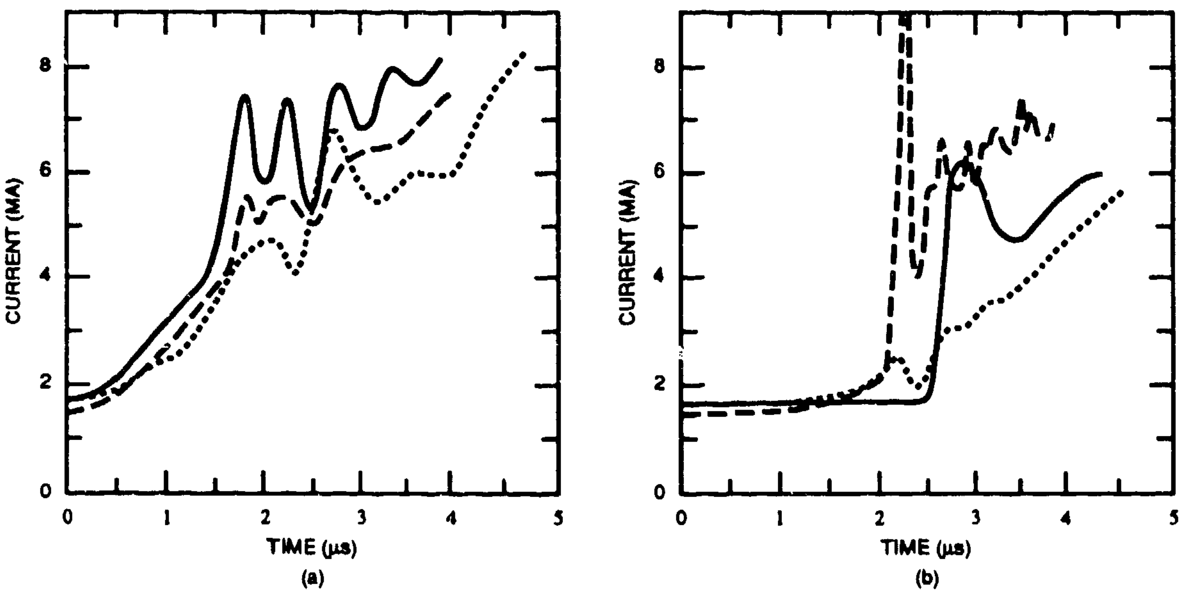

Fig. 4. Integrated dB/dt probe signals as obtained in the MAGO experiment (solid), the computations of [9] (dotted), and MHRDR computations (dashed). The probe of (a) is located in the vicinity of point H of Fig. 1. The probe of (b) is located in the vicinity of point G of Fig. 1.

In spite of the apparent agreement in bulk plasma motion as evidenced by the integrated-dB/dt signals (Fig. 4) and the neutron emitting region, the total computed yield is a factor of 10^{-3} less than the reported yield, even after the fact that deuterium is used in our computations, whereas D-T was used in the experiment, is taken into account. The neutrons are emitted from a very low density, hot plasma which is on the trailing edge of the z-pinch which compresses the bulk of the plasma. The hot, low density component is evidently formed, at least in part, by rapid acceleration of plasma through the nozzle followed by a subsequent deceleration as the plasma collides with the bulk plasma.

Fig. 5 summarizes the temperature distribution and neutron source distribution of the plasma mass. According to Fig. 5b, by 4 μs, 90% of the plasma is above 100 eV, 50% is above 140 eV, and approximately 10% is above 200 eV; at the time of peak neutron yield (2.5 μs), the corresponding temperature values are somewhat less. On the other hand, according to Fig. 5a, 90% of the neutrons are produced by plasma at a temperature well above 200 eV, and when the neutron production rate peaks, 90% of the production comes from plasma above 700 eV. Because the 90% curve of Fig. 5a is in general well above the 10% curve of Fig. 5b, Fig. 5 indicates that the computed neutron yield originates in much less than 10% of the total plasma mass.

4. OTHER MAGO COMPUTATIONS

We have also initiated computations of the MAGO experiment using the computer code MACH2 [13]. Because MACH2 has a generalized computational mesh capability, it can represent the MAGO geometry much more accurately than MHRDR (Fig. 1). In principle, the physics model used in our MACH2 computations is identical to that used in MHRDR, but it appears that there are important differences in the detailed implementations. As one example, the resistivity used in MACH2 at 0.025 eV is such that currents will flow at the insulator and in the nozzle region without the need to establish a conducting path, as in MHRDR.

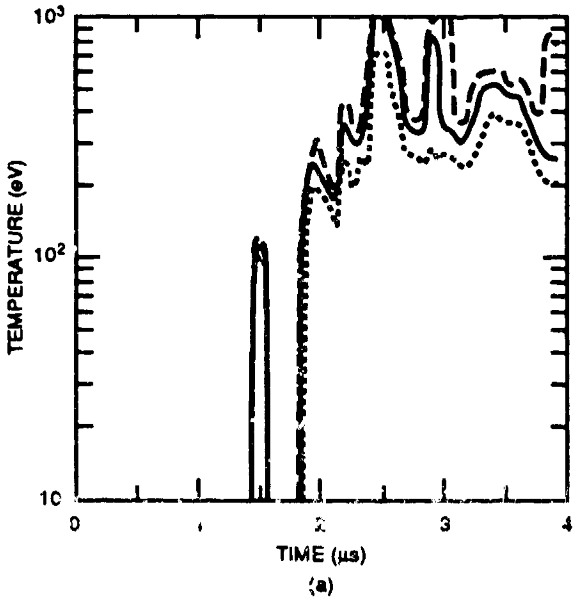

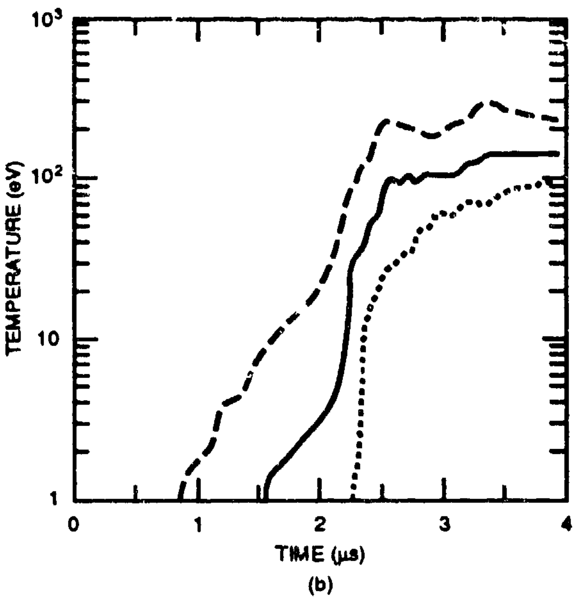

Fig. 5. Temperature distribution of neutron emitting plasma (a) and total plasma mass (b). In (a), 10% (dashed), 50% (solid), and 90% (dotted) of the neutrons are emitted by plasma having a temperature above the value plotted. In (b), 10% (dashed), 50% (solid), and 90% (dotted) of the total plasma mass has a temperature above the value plotted.

Although some numerical difficulties have been encountered in our MACH2 attempts, our most successful computation completed to date is in qualitative agreement with the MHRDR results discussed above. MACH2 also predicts that there are two components of plasma flow, that initiated by current in the nozzle region which compresses the plasma of the second chamber and that initiated by the inverse pinch which rapidly accelerates plasma through the nozzle. MACH2 also predicts that the neutrons are produced by a hot, low density plasma component.

Although MACH2 and MHRDR agree qualitatively, there are important, yet unresolved differences in the quantitative aspects, such as energy coupled to the plasma and the relative importance of the various heating and cooling mechanisms. In addition, the total neutron yield obtained in the MACH2 computation is 10^{-7}-10^{-6} lower than the observed yield.

Eddleman [14] has also performed some MAGO computations. He has interpreted the paper [9] differently and consequently uses a different geometry (dotted geometry of Fig. 1) than used in MHRDR and MACH2. In addition, Eddleman uses an initial temperature of 2 eV, so that the entire gas within the discharge chamber has a relatively high electrical conductivity initially. The basic features of the plasma flow observed in the Eddleman computations are not unlike those observed in MHRDR and MACH2 computations. However, Eddleman obtains much better agreement with the experimentally observed neutron yield.

5. OTHER MTF POSSIBILITIES

In addition to our modeling of MAGO, we are performing computations of other MTF plasma formation and implosion concepts which are based upon fiber-initiated z-pinches. Rapid expansion and instability growth in high-current deuterium-fiber initiated z-pinches [11] has so far prevented such pinches from reaching fusion conditions. However, from an MTF perspective, such unstable behavior may actually be desirable as a means of filling an implosion chamber with hot magnetized plasma. We speculate, but have not yet shown computationally, that an unstable, expanding plasma will settle into a Kadomtsev-stable density profile once it contacts the containing vessel.

A related concept is the implosion of an initially solid deuterium shell on a fiber-initiated z-pinch. We have performed a two-dimensional simulation of a 10-μm-thick deuterium shell having a 1-cm radius surrounding a 30-μm-diameter deuterium fiber and driven by a 10 MA, 40 ns current pulse. This differs somewhat from Park's concept [15], because current is not initially flowing in the fiber. Our simulations show that some portion of the current in the shell transfers to the fiber for preheat and magnetization prior to shell contact with the fiber. Kilovolt temperatures, high densities ($10^{21}/cm^3$), and high magnetic fields (6 MG) over a 2-mm radius approach the MTF regime of enhanced magnetic insulation.

The total mass in the simulation (1 mg) is about the same as in SATURN imploding annular gas-puff experiments [16] and the neutron yield is similar (approximately 10^{12}), suggesting that the fiber pinch at the center may not be a significant factor in the simulation neutron yield. Variation of the masses of fiber and shell, and in the driving current, may make it possible to optimize the fusion yield, by raising the fiber target temperature and density and by providing optimum feed mass from the shell.

6. CONCLUDING REMARKS

In this paper we have concentrated on our computations of the MAGO experiment [9]. MAGO is of interest not only as a possible MTF plasma source suitable for subsequent implosion but also in its own right as a unique plasma device which gives a very interesting neutron yield.

Although all computations we have discussed in this paper give qualitatively similar bulk plasma behavior, there are important quantitative differences which we are attempting to resolve. Some differences are expected to be attributed to physics model considerations (e.g., resistivity, initial conditions) and to geometry. However, it is likely that many of the differences will be atrributed to differences in numerical techniques. All computations agree that the neutrons come from a hot, low density plasma. Historically, the satisfactory numerical treatment of a low density plasma, especially one trailing a main discharge, has presented severe problems, problems which are often overcome only by very "ad hoc" means (e.g., "cutoff" or "floor" values) chosen for computational convenience, not accuracy. We know that each of the codes we have discussed use different techniques for low density plasma. We also know that each code has used different zoning resolution, and it is interesting to note that the best prediction of yield [14] is the most coarsely zoned, whereas the lowest predicted yield (MACH2) used the finest resolution.

We have not yet completed MAGO computations using the complete physics treatments available to us. Clearly, a trivial refinement to our computations would be the use of D-T rather than deuterium. A second refinement would be to use a "two-temperature" model. Initial MHRDR computations suggest that the ions may be more than a factor of 3 hotter than the electrons in the low density plasma at the time of peak yield. We have not performed computations with sufficient zoning resolution to observe possible magnetically driven Rayleigh-Taylor instabilities, for example, in the nozzle region or in the z-pinch of the main chamber.

MAGO is of interest as a candidate for producing the initial preheated and magnetized plasma required in an MTF system. We have not yet evaluated whether or not the MAGO plasma is suitable for subsequent implosion and we have not yet evaluated whether or not it is possible to build an implosion system suitable for imploding the MAGO plasma.

REFERENCES

[1] V. N. Mokhov, V. K. Chernyshev, V. B. Yakubov, M. S. Protasov, V. M. Danov, and E. I. Zharinov, "A Possible Solution of the Controlled Thermonuclear Fusion Problem Based on Magnetogasdynamic Energy Storage," *Sov. Phys. Dokl.*, Vol 24, 1979, pp. 557-559.

[2] R. C. Kirkpatrick, I. R. Lindemuth, R. E. Reinovsky, M. S. Ward, "Parameter Space for Magnetized Target Fusion," this conference.

[3] I. R. Lindemuth and R. C. Kirkpatrick, "Parameter Space for Magnetized Fuel Targets in Inertial Confinement Fusion," *Nuclear Fusion*, Vol 23, 1983, pp. 263-284.

[4] I. R. Lindemuth, R. C. Kirkpatrick, "The Promise of Magnetized Fuel: High Gain in Inertial Confinement Fusion," *Fusion Technology*, Vol. 20, 1991, pp. 829-833.

[5] R. C. Kirkpatrick, I. R. Lindemuth, "Ignition and Burn in Inertially Confined Magnetized Fuel," *Fusion Technology*, Vol. 20, 1991, pp. 834-837.

[6] V. K. Chernyshev, B. E. Grinevich, V. V. Vakrushev, V. I. Mamyshev, "Scaling Image of 90MJ Explosive Magnetic Generators," in *Megagauss Fields and Pulsed Power Systems (Megagauss-V)* (V. Titov, G. Shvetsov, Ed.), New York: Nova Science Publishers, 1990, pp. 347-350.

[7] A. I. Pavlovskii, R. Z. Lyudaev, B. A. Boyko, A. S. Boriskin, A. S. Kravchenko, V. E. Gurin, V. I. Mamyshev, "Investigation of Disc Magnetocumulative Generators," in *Megagauss Fields and Pulsed Power Systems (Megagauss-V)* (V. Titov, G. Shvetsov, Ed.), New York: Nova Science Publishers, 1990, pp. 331-336.

[8] R. E. Reinovsky, I. R. Lindemuth, S. P. Marsh, "Future Explosive Pulse-Power Technology for High-Energy Plasma Physics Experiments," in *Digest of Technical Papers: Proc. VIII IEEE Pulsed Power Conf.* (R. White and K. Prestwich, Ed.), New York: Institute of Electrical and Electronics Engineers, 1991, pp. 415-418.

[9] A. M. Buyko, G. I. Volkov, S. F. Garanin, V. A. Demidiov, Yu. N. Dolin, V. V. Zmushko, V. A. Ivanov, V. P. Korchagin, M. V. Lartsev, V. I. Mamyshev, I. V. Morozov, V. N. Mokhov, N. N. Moskvichev, A. P. Mochalov, E. S. Lavlovskiy, S. V. Pak, S. V. Trusillo, V. K. Chernyshev, V. B. Yakubov, "Investigation into the Possibility of Obtaining Thermonuclear Magnetized Plasma in a System with Magnetic Compression--MAGO," to be published in the Proceedings of the Third Zababakhin Scientific Talks, Kistym, Russia, January, 1992.

[10] I. R. Lindemuth, "Two-Dimensional Behavior of Megagauss-Field-Confined Solid Fiber Z-Pinches," in *Megagauss Fields and Pulsed Power Systems (Megagauss-V)* (V. Titov, G. Shvetsov, Ed.), New York: Nova Science Publishers, 1990, pp. 275-280.

[11] P. T. Sheehey, J. E. Hammel, I. R. Lindemuth, D. Scudder, J. S. Shlachter, R. Lovberg, R. Riley, "Two-Dimensional Direct Simulation of Deuterium-Fiber-Initiated Z-Pinches with Detailed Comparison to Experiment," *Physics of Fluids B*, Vol. 4, 1992, pp. 3698-3706.

[12] J. V. Parker, Los Alamos National Laboratory private communication, 1992.

[13] J. Buff, M. H. Frese, A. J. Giancola, R. E. Peterkin, Jr., "Simulations of a Plasma Flow Switch," *IEEE Transactions on Plasma Science*, Vol. 15, 1987, p. 766.

[14] J. L. Eddleman and C. W. Hartman, "2D MHD Modeling of the MAGO Experiment," this conference.

[15] P. B. Parks, "Magneto-Inertial Fusion," in Physics of Alternative Magnetic Confinement Schemes (S. Ortolani, E. Sindoni, Ed.), Bologna, Italy: Editrice Compositori, 1991, pp. 1083-1090.

[16] D. H. McDaniel, M. K. Matzen, E. J. McGuire, T. J. Nash, R. B. Spielman, J. Seamen, S. F. Lopez, J. S. McGurn, L. Ruggles, T. L. Gilliland, D. Jobe, M. Vargas, "A Review of Z-Pinch Driven Physics Experiments at Sandia National Laboratories," to be published in *Beams '92: Proceedings of the 9th International Conference on High-Power Particle Beams*, Washington, DC, May, 1992.